

Self-ordering on vicinal Si(111) during molecular beam epitaxy

Hiroo Omi* and Yoshikazu Homma†

NTT Basic Research Laboratories, NTT Corporation, Atsugi, Kanagawa 243-0198, Japan

(Received 8 June 2005; revised manuscript received 26 September 2005; published 14 November 2005)

Surface patterns on vicinal Si(111) miscut toward the $[11\bar{2}]$ direction during homoepitaxial step-flow molecular beam epitaxy were investigated by atomic force microscopy and cross-sectional transmission electron microscopy as a function of growth thickness, miscut angle, and growth temperature. We found a one-dimensional universal periodicity of surface patterns after about 200-nm-thick homoepitaxial growth on the vicinal surface at the growth temperature between 700 and 780 °C, which is independent of miscut angle. We discuss the possibility that the growth induced long-range ordering caused by faceting through a energetic balance between (7×7) terraces and (1×1) step-bunched quasifacets on the growing surface.

DOI: [10.1103/PhysRevB.72.195322](https://doi.org/10.1103/PhysRevB.72.195322)

PACS number(s): 68.55.-a, 68.35.Bs, 68.35.Md, 68.37.Ps

I. INTRODUCTION

Nanoscale surface patterning on semiconductor has attracted much attention in the past two decades.¹⁻¹² Self-organization or self-ordering phenomena driven by thermodynamics and kinetics effects on the surface has great potential for nanoscale surface patterning.⁴ Of particular interest in the self-ordering and self-organization is the creation of a periodic array of one-dimensional (1D) structures on Si(111), since such structures can be used as templates for the linear alignment of nanostructures such as nanowires and nanodots.⁸ Indeed, such a 1D periodic structure has been obtained on vicinal Si(111) miscut towards the $[11\bar{2}]$ direction in ultrahigh vacuum via the faceting transition through the transition temperature between (7×7) and (1×1) phases.⁹⁻¹¹ According to previous works,^{1,4-9} the surface pattern is composed of periodic alternative arrays of (7×7) terrace and (1×1) step-bunched quasifacet structures, and the periodicity is determined by the competition between elastic relaxation energy and domain boundary energy on the vicinal Si(111) under a thermal equilibrium condition. In principle, therefore, if one could manipulate these energies, it should be possible to control the periodicity of 1D patterns for subsequent nanostructure self-assembly. However, in practice, it is difficult to control them by thermal annealing alone.⁸⁻¹⁰ Consequently, only one universal periodicity has been observed on vicinal Si(111).

In addition to using faceting on the surface, the approach using surface kinetics and a combination of surface kinetics and thermodynamics on a surface is promising. In this approach, 1D surface patterns are usually formed using step-bunching phenomena during growth, sublimation, metal adsorption, and direct current heating, and combinations of them on the vicinal Si(111) surface.^{2,11,12} In step-bunching during growth, generally, growth kinetics on the vicinal surface play important roles, meaning that the 1D periodicity can be tuned by controlling the processes of growth kinetics in homoepitaxial growth.¹³⁻¹⁶ In heteroepitaxial step-flow growth, particularly, stress is another important parameter for forming uniform surface patterns.¹⁷

In the context of this line of thinking, it has been demonstrated that step-bunching formation succeeds in producing

periodic arrays of step bunches on the vicinal GaAs(001) during homoepitaxial growth and on vicinal Si(001) during SiGe heteroepitaxial growth.¹⁸ However, surface patterning on Si(111) via homoepitaxial step-flow growth in molecular beam epitaxy (MBE) has rarely been explored and 1D self-organization has not been reported yet.¹⁹⁻²³ Most of the work on Si(111) has focused on island growth and layer-by-layer growth of Si on Si(111) in order to gain an understanding of the growth mechanism on an atomic scale. Thus, the initial stage of the growth was of primary interest.^{3,24,25} As for the step pattern formation on vicinal Si(111) miscut toward the $[11\bar{2}]$ direction during step-flow growth, some researchers have reported that the step arrangement strongly depends on the growth thickness, the growth temperature, and substrate miscut angle.¹⁵ Yokohama *et al.*¹⁹ reported step arrangement on vicinal Si(111) after several-nanometers-thick step-flow growth between 400 and 500 °C. Omi and Ogino have found a two-dimensional ordering in step patterns after 150-nm-thick Si step-flow growth on vicinal Si(111) at the growth temperature between 500 and 600 °C.²² Hibino *et al.* have reported that step bunches were formed on vicinal Si(111) after thin (<20 nm) step-flow growth between 600 and 750 °C.²⁰ We have also reported that Si step-flow growth proceeds as it does on Si(113) at the growth thickness below 10 nm at 700 °C. However, it is not clear whether ordering of step bunches happen on vicinal Si(111) after thicker (>20 nm) growth at temperatures above 700 °C.

In this work, we studied surface pattern formations during Si molecular beam epitaxy on Si(111) miscut toward the $[11\bar{2}]$ direction as a function of growth thickness, miscut angle, and growth temperature using ex-situ atomic force microscopy and cross-sectional transmission electron microscopy. We discovered the spontaneous formation of a new universal periodicity in surface patterns on the vicinal Si(111) during homoepitaxial step-flow growth up to about two hundreds of nanometer thick at growth temperatures of 700 and 780 °C. The regular surface patterns are composed of a periodic array of step-bunched quasi-facets and terraces, and the periodicity is universal in length, which is independent of the miscut angle. We discuss the possibilities that the surface ordering originates from faceting through a new balance of surface free energies on the growing vicinal Si(111).

II. EXPERIMENTS

Experiments were carried out using an MBE chamber equipped with a reflection high-energy electron diffraction (RHEED) apparatus. Si was deposited using a 10-kV electron-beam evaporator. Substrates were heated by a W filament placed behind the sample. Substrate temperature was measured with a pyrometer within ± 20 °C. The thickness of Si thin film was measured with quartz-crystal monitors calibrated by using RHEED oscillations during homoepitaxial growth on Si(111). The ultimate pressure of the chamber was 4×10^{-11} Torr and the pressure during Si deposition was below 3×10^{-9} Torr.

Substrates were vicinal Si(111) wafers (B-doped, 20–30 Ω cm). The substrates were miscut 1.0° , 1.63° , 2.0° , or 4.0° to the $[11\bar{2}]$ direction. They were initially cleaned by repeated oxidation in $\text{H}_2\text{O}_2:\text{H}_2\text{SO}_4$ (1:4) and oxide removal in HF solution, and protective oxides were formed using $\text{HCl}:\text{H}_2\text{O}_2:\text{H}_2\text{O}$ (1:1:5) solutions at the final stage. After outgassing under ultrahigh vacuum at 630 °C for 1–2 hours, the samples were heated up to the (7×7) - (1×1) transition temperature of 860 °C to remove the protective oxides. Then, the Si epitaxial layers were grown on the Si(111) at the growth rate of 0.6 ± 0.1 nm/min and at substrate temperatures between 600 and 780 °C. The thickness of the epitaxial layers was less than 180 nm. After the homoepitaxial growth, (7×7) RHEED patterns on the surface were checked and then the samples were immediately cooled to room temperature. The surface morphology was observed by tapping-mode AFM in air. Cross-sectional transmission electron microscopy (XTEM) was used at the incident energy of 300 keV. Before the XTEM observation, 20-nm-thick amorphous silicon layers were grown on the epitaxial layers on the vicinal Si(111) at room temperature in UHV to maintain the growth induced surface patterns in the interface.

III. RESULTS AND DISCUSSION

Figures 1(a)–1(d) show AFM images from the vicinal Si(111) with miscut angle of 1.63° before and after 10-, 70-, and 180-nm-thick homoepitaxial growth at the substrate temperature of 700 °C. Before growth, as seen in Fig. 1(a), the surface had a 1D pattern composed of alternating terraces and step-bunched quasifacets. The periodicity of the 1D surface pattern was about 70 ± 10 nm, which is in good agreement with the previously observed universal periodicity.^{9–11} The homoepitaxial growth, however, significantly changed the surface pattern as the growth thickness increased. The step-bunched quasifacets on the surface grew during the growth, as seen in the AFM image obtained after 10-nm-thick growth [Fig. 1(b)], making the periodicity of 1D surface pattern larger. In addition, it can be seen clearly that single steps and step bunches [marked by arrows in the Fig. 1(b)], crossed the neighboring step-bunched quasifacets. The presence of the crossing steps indicates that the homoepitaxial step-flow growth on the Si(111) proceeds via the zipping motion of the steps as was observed on Si(113),²⁶ which indicates that the step-bunched quasifacets grow by incorporating the crossing steps at the contact points as indicated by

white arrows in Fig. 1(b). After 70-nm-thick-growth, it is evident that the periodicity of the 1D surface pattern was still becoming larger, but step-bunched quasifacets started to meander with wavelength of about $1 \mu\text{m}$ [Compare the cross-sectional profiles in Figs. 1(a)–1(c)]. Further growth of the 110-nm-thick Si layers resulted in periodic array of meandering terraces and step-bunched quasifacets on the surface [Fig. 1(d)]. To qualitatively analyze the surface periodicity of the 180-nm-thick Si(111), an additional two-dimensional Fourier transformation was done on the AFM image. The analysis shows that the surface pattern prefers a periodicity of about 130 nm along the $[11\bar{2}]$ direction even though the surface has a meandering feature normal to the $[11\bar{2}]$ direction, which indicates that the surface was apparently one-dimensionally self-organized along the $[11\bar{2}]$ direction. Also, several single steps and step bunches were observed to be crossing the terraces neighboring step-bunched quasifacets in Figs. 1(b) and 1(c).

To see more details of thickness dependence and the surface ordering on the -1.63° -miscut Si(111), we plotted average surface periodicity L as a function of growth thickness (Fig. 2). Here, we defined the surface periodicity as the terrace width plus the neighboring step-bunched quasifacets along the $[11\bar{2}]$ direction on the Si(111). As seen in Fig. 2, the surface periodicity increased proportionally with the growth time in the log-log plots below the point indicated by the arrow.²¹ Above the point, however, the periodicity started to saturate, meaning that the growing surfaces were regulated to become ordered after the about two hundreds of nanometer thick Si growth at 700 °C. The periodic pattern formation is thus limitedly observed, which is in contrast to usual step bunching phenomena in growth,²⁶ but similar to the groove formation via faceting on Si(113).²⁷

Figure 3 shows an XTEM image from the 180-nm-thick epitaxial layers on vicinal Si(111). From the image, the angle θ between the step bunch and the terrace was determined to be 10.0° . The facet angles were the same for the 3-nm and 5-nm heights of the step-bunched quasifacet. The XTEM results support the idea that the 1D surface pattern is driven by faceting of (7×7) terraces and (1×1) step-bunched quasifacets during growth. Additionally, the detailed analysis of the image showed that the step-bunched quasifacets are composed of single-BL-height steps, indicating that there is no transition from a single- to a double-bilayer step in the step-bunched quasifacet. This is in contrast to the thermal annealing case, where single-bilayer steps are transformed into double-bilayer steps on the step-bunched quasifacet.¹¹

To investigate the dependence of the miscut angle on the growth-induced step pattern formation, similar experiments were done on the Si(111) as a function of miscut angle. Figure 4 shows the miscut-angle dependence of the periodicity of surface patterns obtained on Si(111) after Si epitaxial layer was grown to a thickness of hundreds of nanometers on the Si(111) with miscut angles of 1.0° , 1.63° , 2.0° , or 4.0° . Shown in the inset are the size distributions of the surface periodicity on the as-grown surface for the 1.63° and 4.0° miscut Si(111), which indicates that the surface prefers to order in a long range along the $[11\bar{2}]$ direction. The average periodicity on the surfaces of the Si(111) with various miscut

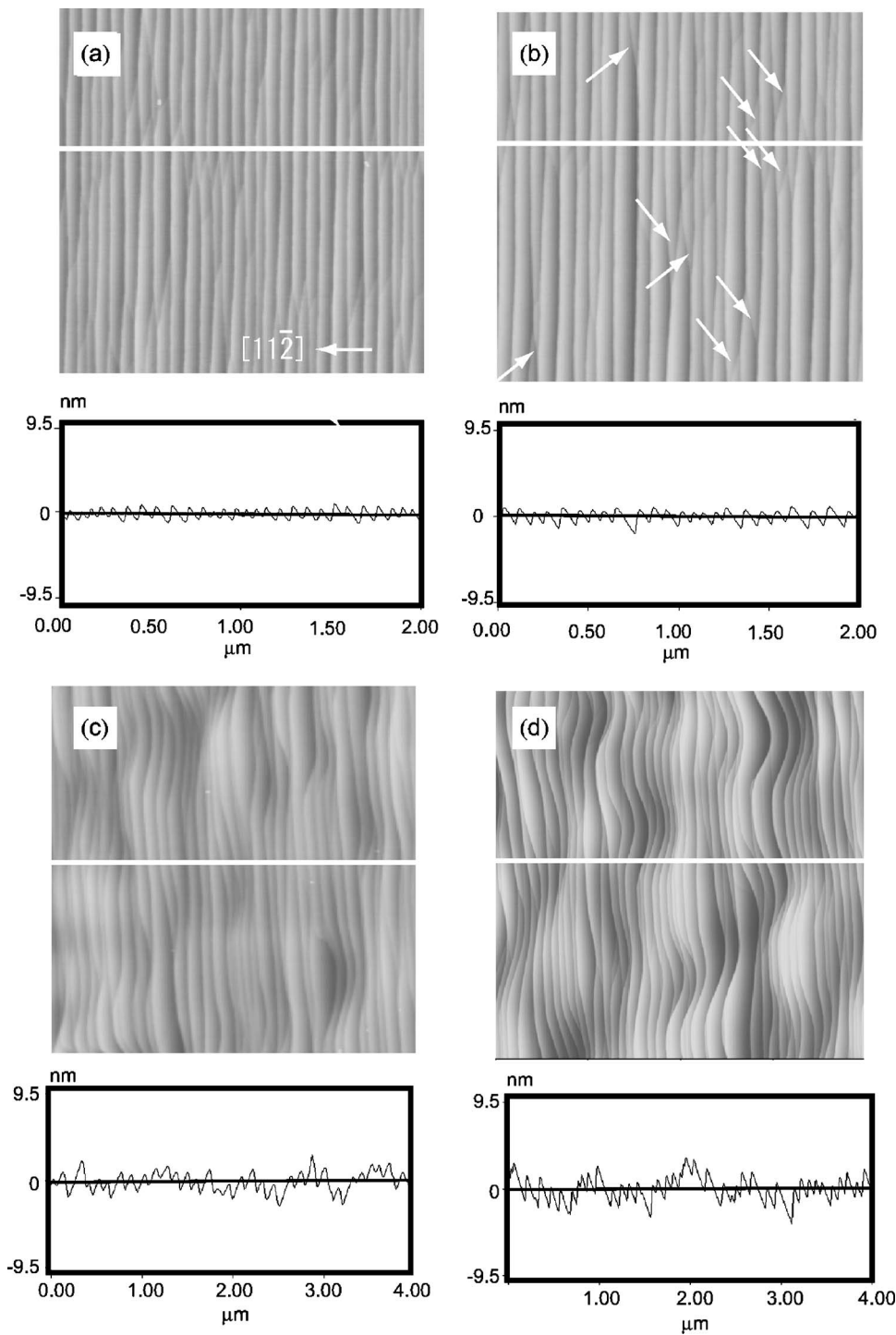


FIG. 1. Representative AFM images of the 1.63°-miscut-Si(111) obtained before and after (a), 10-nm-thick (b), 70-nm-thick (c), and (d) 180-nm-thick silicon deposition at a substrate temperature of 700 °C. The white arrows in (b) indicate single steps and step bunches that cross between neighboring step-bunched quasifacets. Cross-sectional profiles are obtained along the white lines in the figures.

angle is estimated to be 126 ± 8 nm, which was derived from peak position of the Gaussian distribution fit to the experimental data as shown in the inset. The average periodicity is in good accordance with that obtained from the first Fourier transform (FFT) analyses of the AFM images (not shown here). It is apparent that, as can be seen in Fig. 4, the growth-induced surface patterns have an identical periodicity of $L_0^{growth} = 126$ nm irrespective of the miscut angle. The miscut-angle-independence coincides with the case of faceting via transition from (7×7) to (1×1) phases,⁶⁻⁸ where the periodicity L^{anneal} is $60 \text{ nm} \pm 10 \text{ nm}$. The most remarkable differ-

ence between the values of L^{growth} and L^{anneal} is that the periodicity after thick Si growth was twice that obtained after thermal annealing. (Compare the solid and dotted lines in Fig. 4.) This miscut independence strongly indicates that the elastic mechanism limits the periodicity of surface patterns. Possible origins of the periodicity difference are discussed later.

Additionally, we confirmed that increasing the growth temperature to 780 °C did not change the periodicity on the 1.63°- and 4.0°-miscut Si(111). Therefore, it can be said that the surface pattern really preferred to align with the period-

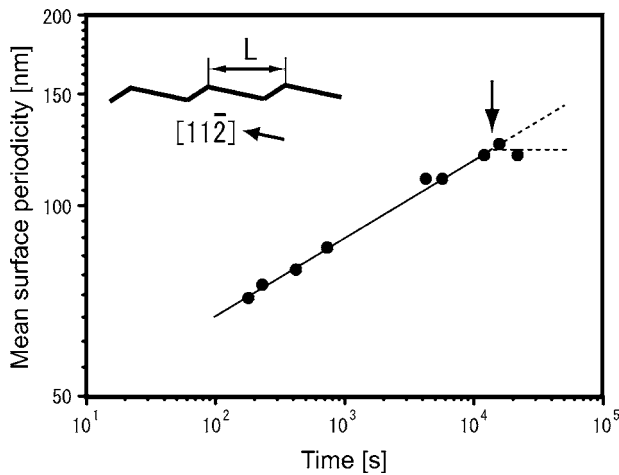


FIG. 2. Time dependence of the average terrace width of growing vicinal Si(111). The increase in surface periodicity saturates at the point indicated by the arrow in Fig. 1. The periodicity L is defined as shown in the inset. The dashed lines are guides for the eyes.

icity after the thick growth independent of the miscut angle and the growth temperature between 700 and 780 °C and that there was a growth-induced universal periodicity of 126 nm. It should be noted here that the growth-induced universal periodicity is limited after the growth of Si epitaxial layers to a thickness of hundreds of nanometers, which suggests that the large amount of mass transport is required in order to attain thermal equilibrium in the growth-induced faceting on Si(111) at the growth temperature of 700 °C.

The 1D ordering on the growing surface can be explained in an analogy to the faceting via the (7×7) - (1×1) transition on vicinal Si(111): According to Refs. 5–7 and 11, the periodicity on Si(111) obtained via the faceting is determined by competition between the reduction of the surface-stress-induced elastic energy in the bulk and the energetic cost of maintaining the edges of the facets.^{5–7,9,11} Men *et al.* predicts that

$$L = \pi a_0 \left[\sin \left(\frac{l}{L} \pi \right) \right]^{-1}, \quad (1)$$

where L is the periodicity and l is the facet width. Here, $a_0 = a \exp[1 + (2\gamma_{anneal}/c\Delta\tau_{anneal}^2)]$, where $\Delta\tau_{anneal} = (\tau_{anneal}^{7 \times 7} - \tau_{anneal}^{1 \times 1})$ is the difference in surface stress between (7×7) and the step-bunched quasifacet, c the elastic constant in the case of the anneal, γ_{anneal} the energy cost for forming the edge of the facet in thermal annealing, and a is a cutoff

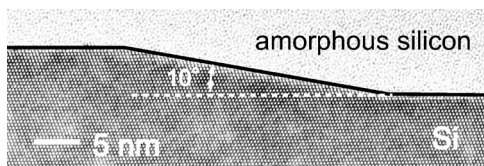


FIG. 3. Cross-sectional transmission electron microscopy image from the 180-nm-thick Si epitaxial layers grown on the 1.63°-miscut Si(111) at the substrate temperature of 700 °C.

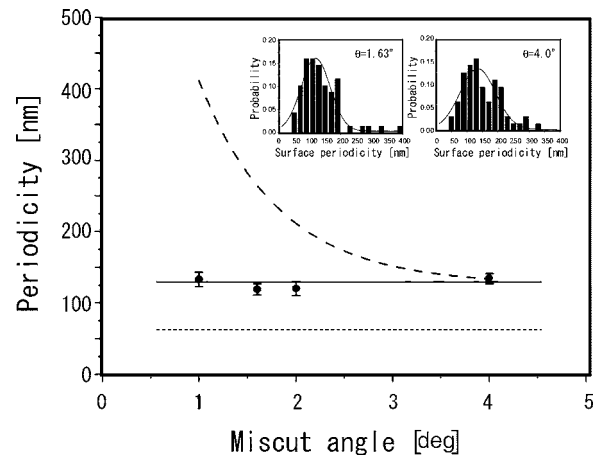


FIG. 4. Miscut dependence of mean surface periodicity L obtained on Si(111) after hundreds of nanometers thick homoepitaxial step-flow growth. The insets show the distributions of surface periodicity on the as-grown Si(111) with miscut angles of 1.63° and 4.0°. Gaussian fits to the distributions are indicated by solid lines in the insets. The solid line indicates the average terrace width obtained by the fit is 126 ± 8 nm. As a reference, we drew the universal periodicity obtained by thermal annealing of Si(111) in UHV (dotted line). The dashed line shows the dependence of periodicity on a miscut angle when the faceting transition is not mediated by elastic relaxation on the surface.

constant on the order of the (7×7) unit-cell lattice constant.¹¹ They found that universal periodicity L_0^{anneal} is 63.5 nm independent of the miscut angle, where $L_0^{anneal} = \pi a_0$, as show in Fig. 4. In the faceting, in addition, they found that periodic ordering starts at $l=L/2$ and that the one-half domain population clearly explains the miscut independence of periodicity using Eq. (1). In the case of growth, similarly, we observed universal periodicity $L_0^{growth} = 126$ nm, which was also independent with the miscut angle (see Fig. 4). Accordingly, our finding indicates that the growth-induced-periodicity does not depend on l/L in the sine term of Eq. (1) and thus the term should be constant.

That the l/L is constant in the growth is also supported by the following experimental results. If surface patterns had formed directly without the faceting transition mediated by the elastic relaxation, the energy minimization with respect to periodicity (L) under the constraint of a constant facet ($\phi=10.0^\circ$) would lead to the following relationship between periodicity and miscut angle: (θ) , $L = L_0^{growth} \{ \sin[(\tan \theta / \tan \phi) \pi] \}^{-1}$.¹¹ Then, the periodicity would have decreased drastically with increasing miscut angle. Using the values of θ and ϕ , we plotted the periodicity in Fig. 4. The value of l/L stays constant irrespective of the miscut angle, which supports idea that the faceting is mediated by elastic relaxation between (7×7) terraces and (1×1) step-bunched quasifacets. Since the faceting transition is identical in the both cases, it is therefore reasonable to consider that the growth induced ordering starts when the populations of the terraces and step-bunched quasifacets are equal, i.e., $l/L=0.5$, in the growth.

On the basis of the above considerations, using Eq. (1), the universal periodicity L_0^{growth} in the growth is determined by

$$L_0^{growth} = \pi a \exp[1 + (2\gamma_{gr}/c\Delta\tau_{gr}^2)], \quad (2)$$

where $\Delta\tau_{growth}$ is the difference in surface stress between (7×7) and the step-bunched quasifacets and elastic constants, γ_{growth} is the energy cost for forming the edge of the facet in the growth, and c is related to the elastic constant on the surface. From Eqs. (1) and (2), we derive the following equations using $L_0^{growth}=126$ nm and $L_0^{aneal}=63.5$ nm:

$$(A) \quad \Delta\tau_{growth}/\Delta\tau_{aneal} = 0.63 \quad \text{if } \gamma_{aneal} = \gamma_{growth}$$

or

$$(B) \quad \gamma_{growth}/\gamma_{aneal} = 2.50 \quad \text{if } \Delta\tau_{aneal} = \Delta\tau_{growth}.$$

For the case of (A), we assume that $\gamma_{aneal} = \gamma_{growth}$. This assumption is reasonable because the edge structure of a (7×7) terrace and that of a (1×1) step-bunched quasifacet are expected to be equal in the case of growth and anneal because the top edges of the steps are usually formed by rows of corner holes of the (7×7) unit cell.¹⁰ Previous works have reported $\Delta\tau_{an}$ of 0.030 eV/Å² (Ref. 28) and 0.060 eV/Å².²⁹ Here, we obtained $\tau_{aneal}^{1\times 1}$ of 0.156 eV/Å², or 0.126 eV/Å², since $\tau_{aneal}^{7\times 7} = 0.186$ eV/Å².³⁰

It is well known that the (1×1) surface has a relaxed bulklike structure with random adatoms. Three models have been proposed for the (1×1) surface reconstruction:³¹⁻³³ the (1×1) - 2×2 model, in which adatoms are adsorbed at T₄ site; the (1×1) - 2×2 (faulted) model, in which adatoms are adsorbed at the H₃ site; and the (1×1) - $\sqrt{3}\times\sqrt{3}$ adatom model.³⁰ According to Ref. 33, first-principle calculations showed that the respective surface stresses are 0.129 , 0.147 , and 0.132 eV/Å². Comparing our experimental results and the calculations, $\tau_{aneal}^{1\times 1} = 0.126$ eV/Å² is in good accordance with the calculated values for the three models and the experimental result of $\tau_{aneal}^{1\times 1} = 0.156$ eV/Å² is slightly larger than the calculations. Therefore, we use $\Delta\tau_{aneal} = 0.060$ eV/Å² rather than $\Delta\tau_{aneal} = 0.030$ eV/Å² in the following considerations. In the case of (A), consequently, we derived $\Delta\tau_{growth} = \tau_{growth}^{7\times 7} - \tau_{growth}^{1\times 1} = 0.038$ eV/Å² and thus $\tau_{growth}^{1\times 1} = 0.148$ eV/Å² when we assumed $\tau_{growth}^{7\times 7} = \tau_{aneal}^{7\times 7}$ (the validity of this assumption is described later), which is in fairly good agreement with the calculated value for the (1×1) - 2×2 adatom (faulted) model.³³ The simple estimation clearly shows that the surface stress on a step-bunched quasifacet in the growth is larger than that of a (1×1) step-bunched quasifacet obtained via the (7×7) - (1×1) transition, indicating that the difference in periodicity could originate from the difference in the surface stress of the (1×1) during growth or that after thermal anneal via the (7×7) - (1×1) transition. The increase in the surface stress on the step-bunched quasifacet during growth is reasonable because the concentration of migrating adatoms on the step-bunched quasifacet during the growth should be higher than that on the step-bunched quasifacet during the (7×7) - (1×1) transition.³⁴ From Eq. (2), the edge energy is estimated to be 0.00056 eV/Å with $c = 0.563$ eV²/Å⁴.³⁵ The edge energy is in accordance with the values of 0.001 eV/Å obtained by Phaneuf *et al.*⁹ but it is about one-sixth the value obtained by Men *et al.*¹¹

It should be noted here that there is another possible explanation of the increase of the surface stress in the step-bunched quasifacet. If there is a difference in the angle ϕ between the step-bunched quasifacet and the (111) terrace during annealing and growth, then, according to Ref. 12, it could cause the anisotropy of surface stress with ϕ , meaning that the step-step distance in the quasifacet is different during annealing and during growth and the resulting facets have a difference in surface stress between them. However, we should recall that the universal periodicity obtained via the (7×7) - (1×1) transition does not so seriously depend on the facet angle; for instance, $L_0^{aneal} = 70 \pm 10$ nm at $\phi = 7^\circ$ (Ref. 10) and $L_0^{aneal} = 62.5$ nm at $\phi = 12.7^\circ$.¹¹ Incidentally, in the growth experiment, we observed the $L_0^{growth} = 126$ nm at $\phi = 10.0^\circ$, which is between $\phi = 7$ and 12.7° . The experimental result suggests that the increase of surface stress due to the angle of the step-bunched quasifacet does not seriously depend on the surface periodicity and thus does not sufficiently explain the doubled length of universal periodicity obtained via the (7×7) - (1×1) transition ($L_0^{growth} \approx 2L_0^{aneal}$).

In the above considerations, we simply assumed that surface stress of (7×7) terraces on Si(111) during annealing and growth was identical ($\tau_{growth}^{7\times 7} = \tau_{aneal}^{7\times 7}$), and argued that the increase in surface stress of step-bunched quasifacet is relevant to the difference in surface periodicity between growth and anneal. However, we should check the validity of the assumption of $\tau_{growth}^{7\times 7} = \tau_{aneal}^{7\times 7}$ and/or consider the possibility of the $\tau_{growth}^{7\times 7} \neq \tau_{aneal}^{7\times 7}$ case; that is, surface stress at the (7×7) terraces during growth is different from that during anneal due to a large number of migrating atoms. Here, let us recall that we observed meandering of step-bunched quasifacets at 70-nm- and 180-nm-thick depositions [see Figs. 1(c) and 1(d)]. This meandering should cost energy because it causes an increase in the length of the facet edges. The question is what derives this increase in the step-bunched quasifacet edge length. Here, if we assume that the surface stress on the (7×7) terrace increases during the growth, we can explain the meandering using a 1D analogy of the strain relaxation model proposed by Marchenko⁵ and Alerhand *et al.*⁶ Therefore, under the assumption that increases in surface stress on the (7×7) terrace is relaxed by the meandering of step-bunched quasifacets, we roughly estimate the degree of increase in the strain-related contribution to the Gibbs free energy density, which can be estimated by measuring the radius of a curving step-bunched quasifacet,³⁶ using the Gibbs-Thomson formulation

$$\frac{\Delta G_{str}}{A} = \frac{\beta_n}{R}, \quad (3)$$

where R is the radius of the curvature of the step-bunched quasifacet, and $\Delta G_{str}/A$ is practically equal to the strain-related contribution to the Gibbs free-energy density on an area A . The β_n is the stiffness of step-bunched quasifacet per unit length, where n is the number of steps in the step-bunched quasifacet. From the AFM images, we found that R is larger than about 450 nm and the corresponding bunched-facet quasifacet has 16 bilayer steps. From Ref. 36, the stiffness of bunched steps is estimated to be 1742 meV/Å² at the

growth temperature if $n=16$.²³ As a result, we obtained, from Eq. (3), a $\Delta G_{str}/A$ that is smaller than $0.38 \text{ meV}/\text{\AA}^2$. The point is that the value of $\Delta G_{str}/A$ is 500 times smaller than that of $\tau_{anneal}^{7\times 7}$, which suggests that the small increase in surface stress of the (7×7) terrace can cause the meandering of step-bunched quasifacets and that part of the small excess of surface stress is possibly relaxed by the meandering of step-bunched quasifacets. However, the value is 100 times smaller than the value of $\Delta\tau_{growth}$ ($\tau_{growth}^{7\times 7} - \tau_{growth}^{1\times 1} = 38 \text{ meV}/\text{\AA}^2$), meaning that the assumption that $\tau_{growth}^{7\times 7} = \tau_{anneal}^{7\times 7}$ is valid in the approximation and thus the universal periodicity during growth should mainly originate from the increase of surface stress in step-bunched quasifacets during growth. In other words, if we assume that the migrating atoms on the (7×7) terrace increase the stress on the (7×7) terrace, there is a mechanism whereby the extra stress is partially relaxed by meandering of the step-bunched quasifacets. However, the degree of the increase in the surface stress on the (7×7) terrace, if the stress exists, is too small compared with the degree of $\Delta\tau_{growth}$ that induced the universal surface periodicity by homoepitaxial step-flow growth.

In the case of (B), where we assume that $\Delta\tau_{anneal} = \Delta\tau_{growth}$, on the other hand, edge energy during growth becomes 2.5 times that after thermal annealing treatment. Such high energy is unlikely because the top edges of steps on the step-bunched quasifacet are usually formed by rows of corner holes of the (7×7) unit cell on upper and lower terraces.^{10,11} In addition, as was confirmed from the XTEM image in Fig. 3, the heights of the steps at the upper and lower edges of a step-bunched quasifacet have single-bilayer, not double-bilayer, height. Therefore, it is considered that the edge energy during growth is nearly the same as that in the thermal annealing case.⁹⁻¹¹ Therefore, it is possible to omit case (B).

Finally, let us discuss potential of the self-ordered surface patterns on the Si(111) for the template applications. For

surface patterning, in general, the periodicity of the surface pattern should be controlled in length. However, we observed a unique periodicity on the surface in the case of thermal anneal, as mentioned in the Introduction. The finding of a new universal periodicity in the growth, therefore, is a real demonstration of how we can change the universal periodicity by manipulating the elastic stresses on Si(111). However, further tuning of the surface periodicity to the desired length remains a problem in this approach. Further, it should be noted here that in the growth approach we encountered a new problem: the meandering of step-bunched quasifacets on the surface with wavelength of about $1 \mu\text{m}$, which would make it difficult to apply the 1D ordered surface pattern as a template.

IV. CONCLUSION

We have investigated the self-organization of surface patterns on vicinal Si(111) miscut toward to the $[11\bar{2}]$ direction during homoepitaxial step-flow conditions as a function of growth thickness, miscut angle, and growth temperature. We found that about 200-nm-thick homoepitaxial growth produced periodical arrays of (7×7) terrace and (1×1) step-bunched quasi-facet on vicinal Si(111) at substrate temperatures between 700 and 780 °C independent of miscut angle. The ordering of the surface pattern on the Si(111) is driven by elastic relaxation between the (7×7) terraces and (1×1) step-bunched quasifacets that grow in the homoepitaxial step-flow growth.

ACKNOWLEDGMENTS

We thank Professor Stoyan Stoyanov, Dr. Vesselin Tonchev, and Dr. Hiroki Hibino for stimulating discussions and valuable comments.

*Email address: homi@will.brl.ntt.co.jp

†Present address: Department of Physics, Tokyo University of Science, Kagurazaka 1-3, Shinjuku, Tokyo 162-8601, Japan.

¹H.-C. Jeong and E. D. Williams, Surf. Sci. Rep. **34**, 171 (1999).

²K. Yagi, H. Minoda, and M. Degawa, Surf. Sci. Rep. **43**, 45 (2001).

³B. Voigtländer, Surf. Sci. Rep. **43**, 127 (2001).

⁴S. Rousset, V. Repain, G. Baudot, H. Ellmer, Y. Garreau, V. Etgens, J. M. Berroir, B. Croset, M. Sotto, P. Zeppenfeld, J. Ferré, J. P. Jamet, C. Chappert, and J. Lecoer, Mater. Sci. Eng., B **96**, 169 (2002).

⁵V. I. Marchenko, Pis'ma Zh. Eksp. Teor. Fiz. **33**, 397 (1981) [JETP Lett. **33**, 381 (1981)].

⁶O. L. Alerhand, D. Vanderbilt, R. D. Meade, and J. D. Joannopoulos, Phys. Rev. Lett. **61**, 1973 (1981).

⁷H. J. W. Zandvliet, B. S. Swartzentruber, W. Wulfhekkel, B. J. Hattink, and Bene Poelsema, Phys. Rev. B **57**, R6803 (1998).

⁸A. Sgarlata, D. P. Szuktnik, A. Balzalotti, N. Motta, and F. Rosei, Appl. Phys. Lett. **83**, 4002 (2003).

⁹R. J. Phaneuf, N. C. Bartelt, E. D. Williams, W. Świąch, and E. Bauer, Phys. Rev. Lett. **67**, 2986 (1991).

¹⁰J. Viernow, J.-L. Lin, D. Y. Petrovykh, F. M. Leible, F. K. Men, and F. J. Himpsel, Appl. Phys. Lett. **72**, 948 (1998); J.-L. Lin, D. Y. Petrovykh, J. Viernow, F. K. Men, D. J. Seo, and F. J. Himpsel, J. Appl. Phys. **84**, 255 (1998).

¹¹F. K. Men, F. Liu, P. J. Wang, C. H. Chen, D. L. Cheng, J. L. Lin, and F. J. Himpsel, Phys. Rev. Lett. **88**, 096105 (2002).

¹²J. J. Métois, A. Saúl, and P. Müller, Nat. Mater. **4**, 238 (2005).

¹³Y. Homma and N. Aizawa, Phys. Rev. B **62**, 8323 (2000).

¹⁴H. Minoda, Phys. Rev. B **64**, 233305 (2001).

¹⁵W. F. Chung and M. S. Altman, Phys. Rev. B **66**, 075338 (2002).

¹⁶M. Krishnamurthy, M. Wasserman, D. R. M. Williams, and P. M. Petroff, Appl. Phys. Lett. **62**, 1922 (1993).

¹⁷F. Liu, J. Tersoff, and M. G. Lagally, Phys. Rev. Lett. **80**, 1268 (1998).

¹⁸Y. H. Phang, C. Teichert, M. G. Lagally, L. J. Peticolos, J. C. Bean, and E. Kasper, Phys. Rev. B **50**, 14435 (1994).

¹⁹T. Yokohama, T. Yokotsuka, I. Sumita, and M. Nakajima, Surf.

- Sci. **357–358**, 855 (1996).
- ²⁰H. Hibino and T. Ogino, in *Materials Issues and Modeling for Device Nanofabrication*, edited by L. Merhari, L. T. Wille, K. Gonsalves, M. F. Gyure, S. Matsui, and L. J. Whitman, Mater. Res. Soc. Symp. Proc. No. 584 (Materials Research Society, Pittsburgh, 2000), p. 77.
- ²¹H. Omi and T. Ogino, J. Vac. Sci. Technol. A **17**, 1610 (1999).
- ²²H. Omi and T. Ogino, Thin Solid Films **380**, 15 (2000).
- ²³H. Omi and Y. Homma, Jpn. J. Appl. Phys., Part 2 **43**, L822 (2004).
- ²⁴C. J. Lanczycki, R. Kotlyar, E. Fu, Y.-N. Yang, E. D. Williams, and S. Das Sarma, Phys. Rev. B **57**, 13132 (1998).
- ²⁵J. Mysliveček, T. Jarolímek, P. Šmilauer, B. Voigtländer, and M. Kästner, Phys. Rev. B **60**, 13869 (1999).
- ²⁶K. Sudoh and H. Iwasaki, J. Phys.: Condens. Matter **15**, S3241 (2003).
- ²⁷S. Song, M. Yoon, S. G. J. Mochrie, G. B. Stephenson, and S. T. Milner, Surf. Sci. **372**, 37 (1997).
- ²⁸R. D. Twisten and J. M. Gibson, Phys. Rev. B **50**, 17628 (1994).
- ²⁹J. B. Hannon and R. M. Tromp, J. Vac. Sci. Technol. A **19**, 2596 (2001).
- ³⁰R. E. Martinez, W. M. Augustyniak, and J. A. Golovchenko, Phys. Rev. Lett. **64**, 1035 (1990).
- ³¹S. Kohmoto and A. Ichimiya, Surf. Sci. **223**, 400 (1989).
- ³²Y. Fukaya and Y. Shigeta, Phys. Rev. B **65**, 195415 (2002).
- ³³R. D. Meade and D. Vanderbilt, Phys. Rev. B **40**, 3905 (1989).
- ³⁴According to the calculation by Martinez, Augustyniak, and Golovchenko (Ref. 30), the surface stress of the (5×5) surface, which was often observed on the homoepitaxial islands on Si(111), are $0.221 \text{ eV}/\text{\AA}^2$. The experimental results are also not in accordance with the surface stress of the (5×5) reconstruction.
- ³⁵C. Schwennicke, X.-S. Wang, T. L. Einstein, and E. D. Williams, Surf. Sci. **418**, 22 (1998).
- ³⁶H. Omi, D. J. Bottomley, Y. Homma, T. Ogino, S. Stoyanov, and V. Tonchev, Phys. Rev. B **66**, 085303 (2002).